


Article

Significantly Enhanced Crystallization of Poly(ethylene succinate-co-1,2-propylene succinate) by Cellulose Nanocrystals as an Efficient Nucleating Agent

Siyu Pan, Zhiguo Jiang * and Zhaobin Qiu * 

State Key Laboratory of Chemical Resource Engineering, Beijing University of Chemical Technology, Beijing 100029, China; 2020200319@grad.buct.edu.cn

* Correspondence: jiangzg@mail.buct.edu.cn (Z.J.); qiuzb@mail.buct.edu.cn (Z.Q.)

Abstract: Poly(ethylene succinate-co-1,2-propylene succinate) (PEPS) is a novel aliphatic biodegradable polyester with good mechanical properties. Due to the presence of methyl as a side group, the crystallization rate of PEPS is remarkably slower than that of the poly(ethylene succinate) homopolymer. To promote the potential application of PEPS, the effect of cellulose nanocrystals (CNC) on the crystallization behavior, crystalline morphology, and crystal structure of PEPS was investigated in this research with the aim of increasing the crystallization rate. CNC enhanced both the melt crystallization behavior of PEPS during the cooling process and the overall crystallization rate during the isothermal crystallization process. The crystallization rate of PEPS became faster with an increase in CNC content. The crystalline morphology study directly confirmed the heterogeneous nucleating agent role of CNC. The crystal structure of PEPS remained unchanged in the composites. On the basis of the interfacial energy, the nucleation mechanism of PEPS in the composites was further discussed by taking into consideration the induction of CNC.



Citation: Pan, S.; Jiang, Z.; Qiu, Z. Significantly Enhanced Crystallization of Poly(ethylene succinate-co-1,2-propylene succinate) by Cellulose Nanocrystals as an Efficient Nucleating Agent. *Polymers* **2022**, *14*, 224. <https://doi.org/10.3390/polym14020224>

Academic Editor: Ryan M. Van Horn

Received: 14 December 2021

Accepted: 3 January 2022

Published: 6 January 2022

Publisher's Note: MDPI stays neutral with regard to jurisdictional claims in published maps and institutional affiliations.



Copyright: © 2022 by the authors. Licensee MDPI, Basel, Switzerland. This article is an open access article distributed under the terms and conditions of the Creative Commons Attribution (CC BY) license (<https://creativecommons.org/licenses/by/4.0/>).

Keywords: poly(ethylene succinate-co-1,2-propylene succinate); cellulose nanocrystals; crystallization

1. Introduction

Due to the growing concerns regarding both fossil resource deficiency and environment protection, bio-based and biodegradable aliphatic polyesters have been the research focus, from a sustainable viewpoint, of both the academic and industrial fields in recent decades [1–6]. Poly(ethylene succinate) (PES) is a typical member of bio-based and biodegradable aliphatic polyesters, as the monomers to synthesize PES, i.e., ethylene glycol and succinic acid, may be derived from either fossil resource or bio-based resources. It shows a melting point (T_m) of approximately 103 °C with a glass transition temperature (T_g) of −11 °C; in addition, the tensile mechanical property of PES is comparable to those of low-density polyethylene and polypropylene [7–13]. For instance, it displays a tensile modulus (E_t) of 409 ± 13 MPa, a tensile strength (σ) of 23.4 ± 1.5 MPa, and an elongation at break (ϵ) of $285 \pm 30\%$ [14]. To modify the physical properties and meet various practical application requirements, some PES based copolymers have been synthesized through the copolymerization method by introducing a new linear diol or diacid monomer during the polymerization process of PES [15–20]. With respect to PES, these copolymers usually display lower T_m values and better toughness with higher ϵ values [15–20]. In addition, some novel PES based copolymers with different lengths of side groups have also been synthesized and studied in the literature by the use of some 1,2-diols, such as 1,2-propanediol, 1,2-hexanediol, and 1,2-decanediol, as comonomers [14,21–24]. These novel PES-based copolymers show the same main chain structures as PES, except that some side groups (such as methyl, butyl, and octyl) are randomly linked to the polymer main chain. In a previous study, the effect of different lengths of side groups on the thermal, crystallization, and mechanical properties of PES were systematically investigated [24].

Among these copolymers, poly(ethylene succinate-*co*-1,2-propylene succinate) (PEPS) is of great importance and interest, as the presence of a small amount of the simplest C–H side group of methyl (–CH₃) can lead to a remarkable change of the physical properties of PES [14,24]. For instance, the storage modulus, loss modulus, and complex viscosity of PEPS were significantly higher than those of PES; even the 1,2-propylene succinate (PS) unit was only approximately 5 mol%. In addition, the tensile mechanical property of PEPS was superior to that of PES. For instance, PEPS with roughly 5 mol% of PS unit showed a higher σ of 40.9 ± 4.1 MPa and a higher ϵ of $755 \pm 91\%$, while the σ and ϵ values of PES were only 23.4 ± 1.5 MPa and $285 \pm 30\%$, respectively [14]. Although PEPS showed better rheological and tensile mechanical properties than PES, the crystallization rate of PEPS became slower due to the random copolymer feature. From a practical application viewpoint, the crystallization rate of PEPS should be remarkably enhanced. So far, the use of heterogeneous nucleating agents has been regarded as the most efficient method to accelerate the crystallization of polymer materials because it may both provide sufficient active nucleating sites and reduce the nucleation activation energy barrier of polymer crystallization [7–13,23].

Among the widely used nucleating agents, cellulose nanocrystals (CNC) are of particular interest. The characteristics of CNC are as follows: bio-based, biodegradable, highly crystalline, rod-like, high aspect ratio, and superior mechanical property; in addition, the hydroxyl groups on the surface also provide the possibility of chemical modification to increase the solubility in organic solvent and the compatibility with polymer matrix [25–28]. So far, some CNC nucleated biodegradable polymers have been reported in the literature, such as poly(ϵ -caprolactone) (PCL), poly(L-lactic acid) (PLLA), PES, poly(butylene succinate) (PBS), poly(hexamethylene succinate) (PHS), poly(butylene succinate-*co*-butylene adipate) (PBSA), and poly(ethylene adipate) (PEA) [29–40].

In this research, we prepared low contents of CNC nucleated PEPS composites and extensively studied the effect of CNC as a heterogeneous nucleating agent on the crystallization of PEPS. CNC could induce the melt crystallization of PEPS at a relatively fast cooling rate of 20 °C/min; moreover, CNC remarkably shortened the crystallization time and crystallization half-time of PEPS during the isothermal crystallization indicating the efficient nucleating agent effect. The significance of this study is summarized as follows. On the one hand, PEPS/CNC composites, both of which were biodegradable, were prepared and studied for the first time. On the other hand, CNC significantly accelerated the crystallization of PEPS under different crystallization conditions; moreover, we further reasonably discussed the nucleation mechanism of PEPS induced by CNC on the basis of the interfacial energy. Therefore, this research is important and interesting in the fields of both polymer crystallization and biodegradable polymer composites.

2. Experimental Section

2.1. Materials

PEPS ($M_n = 5.3 \times 10^4$ g/mol, PDI = 1.89, and PS content = 4.1 mol%) was synthesized via a two-stage melt polycondensation reaction in our laboratory [14]. CNC (with an average diameter of 5–20 nm and length of 50–200 nm) was produced by Shanghai ScienceK Nanotechnology Co., Ltd. *N,N*-dimethylformamide (DMF) (purity = 99.5%) was bought from Tianjin Damao Chemical Reagent Factory, China.

The chemical structures of PEPS and CNC are illustrated in Figure 1.

2.2. Preparation of PEPS/CNC Composites

Three PEPS/CNC composites, i.e., PEPS/CNC0.25, PEPS/CNC0.5, and PEPS/CNC1, were prepared in this research, with the number being the wt% of CNC. The preparation procedure of PEPS/CNC1 was simply described as follows. First, PEPS (2.97 g) was dissolved into DMF (35 mL) at 40 °C for 2.5 h, and CNC (30 mg) was dispersed into DMF (15 mL) after a sonication process of 2.5 h. Second, the PEPS solution and the CNC dispersion were mixed together at 40 °C for 4.5 h. Third, the film was obtained after

evaporating DMF at 40 °C for one night in a fume hood and for 7 days in a vacuum oven. Similarly, PEPS/CNC0.25 and PEPS/CNC0.5 were also prepared.

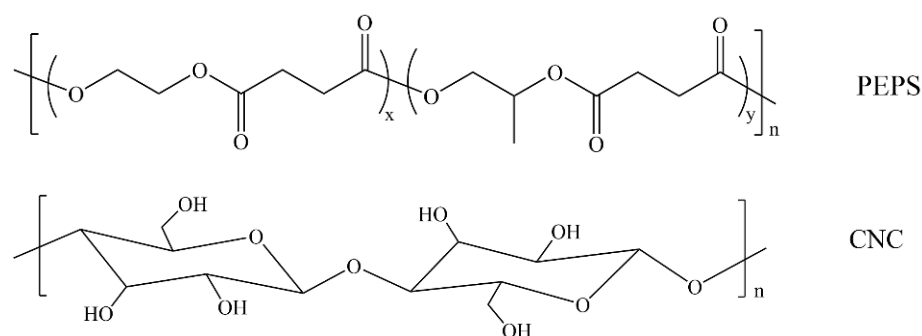


Figure 1. Chemical structures of PEPS and CNC.

2.3. Characterizations

Thermogravimetric analysis (TGA) was performed on a TA instrument Q50 to study the thermal stability of PEPS and PEPS/CNC composites under nitrogen atmosphere at a heating rate of 20 °C/min.

The crystallization behavior of PEPS and PEPS/CNC composites was investigated with a TA Q100 differential scanning calorimeter (DSC) under a nitrogen atmosphere. The weight of each sample was approximately 4~5 mg. For each test, the thermal history of a fresh sample was first eliminated by heating at 40 °C/min to 130 °C (almost 40 °C above the T_m of 93.9 °C for PEPS) and holding there for 3 min. The nonisothermal melt crystallization behavior of PEPS and PEPS/CNC composites was studied at a cooling rate of 20 °C/min after the elimination of the previous thermal history of the samples. In the case of the isothermal melt crystallization kinetics study, the sample was isothermally crystallized at the chosen crystallization temperature (T_c) for sufficient time after cooling from the crystal-free melt at 60 °C/min after the elimination of previous thermal history. In this research, the crystallization was studied in a T_c range from 63 to 71 °C.

A polarized optical microscope (POM) (Olympus BX51) equipped with a hot stage (Linkam THMS 600) was used to observe the spherulitic morphology of PEPS and PEPS/CNC composites.

A Rigaku Ultima IV X-ray diffractometer was operated at 40 kV and 200 mA to study the crystal structures of PEPS and PEPS/CNC composites. The wide-angle X-ray diffraction (WAXD) experiments were performed with a rate of 5°/min at ambient temperature in a 2θ range of 5° to 40°. The samples for the WAXD measurement underwent an isothermal crystallization at 63 °C for 8 h in an oven.

3. Results and Discussion

Thermal decomposition temperature (T_d) is an important physical parameter from the viewpoints of both polymer processing and the long time use at elevated temperatures. The influence of CNC on the thermal stability of PEPS was first explored with TGA at a heating rate of 20 °C/min under a nitrogen atmosphere. Figure 2 demonstrates the TGA curves of PEPS and PEPS/CNC composites, from which one-step thermal decomposition behavior was found for all samples, irrespective of CNC content. The T_d values, corresponding to 5 wt% weight losses, were read from Figure 2, which increased slightly from 338.3 °C for PEPS to about 343.7 °C for the composites. The slight increase in T_d arose from the presence of CNC, which played a role in physical barriers and hindered the heat transfer and permeation of combustion gas in the PEPS matrix [35].

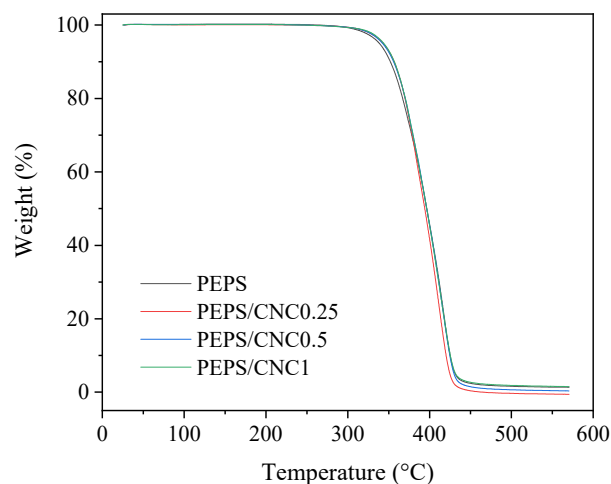


Figure 2. TGA curves of PEPS and PEPS/CNC composites.

Although PEPS has the same main chain structure as PES, the presence of methyl as a side group destroys the regularity of the main chain structure. As a result, the crystallizability of PEPS is remarkably weaker than that of the PES homopolymer. The DSC cooling traces are depicted in Figure 3 for PEPS and PEPS/CNC composites, which were nonisothermally crystallized at a fast cooling rate of 20 °C/min from the crystal-free melt. Under this crystallization condition, PEPS did not crystallize, showing no crystallization exothermic peak in Figure 3. On the contrary, regardless of CNC content, the three PEPS/CNC composites showed obvious crystallization exothermic peaks during the crystallization process, indicating that CNC played an outstanding nucleating agent role and enhanced the crystallization of PEPS. From Figure 3, the melt crystallization temperature (T_{mc}) was determined. The T_{mc} values gradually increased from 28.3 °C for PEPS/CNC0.25 to 29.7 °C for PEPS/CNC0.5 and 35.5 °C for PEPS/CNC1, respectively. Similarly, the melt crystallization enthalpy (ΔH_{mc}) remarkably increased from 21.9 J/g for PEPS/CNC0.25 to 47.1 and 54.6 J/g for PEPS/CNC0.5 and PEPS/CNC1, respectively. By using the equilibrium heat of fusion of PES (180 J/g) [10], the absolute degree of crystallinity values of the three composites was approximately calculated to be 12.2%, 26.2% and 30.3%, respectively. The obvious increase in both T_{mc} and ΔH_{mc} revealed that CNC remarkably enhanced the melt crystallization of PEPS even at a relatively fast cooling rate of 20 °C/min as an efficient nucleating agent.

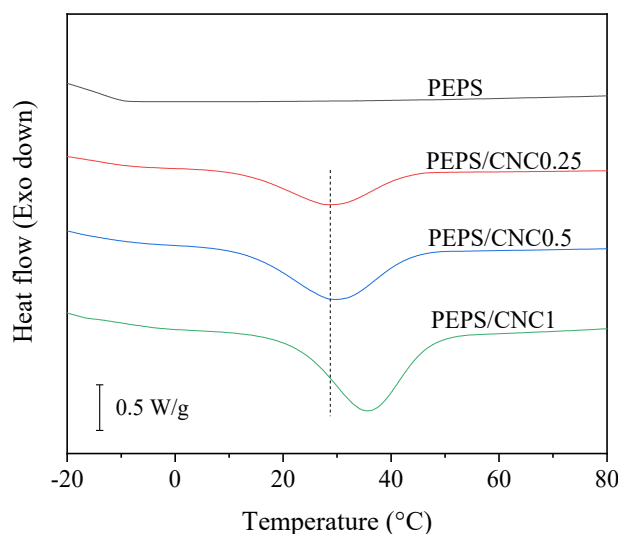


Figure 3. Melt crystallization behavior of PEPS and PEPS/CNC composites at 20 °C/min.

The effect of CNC on the isothermal melt crystallization kinetics of PEPS was further investigated with DSC in this research. Figure 4a show the plots of relative crystallinity versus crystallization time of PEPS and PEPS/CNC composites at a T_c of 71 °C. Due to the small degree of supercooling, PEPS crystallized slowly and required 87.8 min to complete the crystallization, while the total crystallization time for PEPS remarkably became shorter in the composites. For instance, PEPS/CNC0.25 needed 29.6 min to finish the crystallization, while PEPS/CNC1 even only required 18.2 min at the same T_c , suggesting that the higher the CNC content, the shorter the crystallization time. The significantly short crystallization time of PEPS/CNC composites indicated that the isothermal melt crystallization of PEPS was also promoted by CNC as an effective nucleating agent.

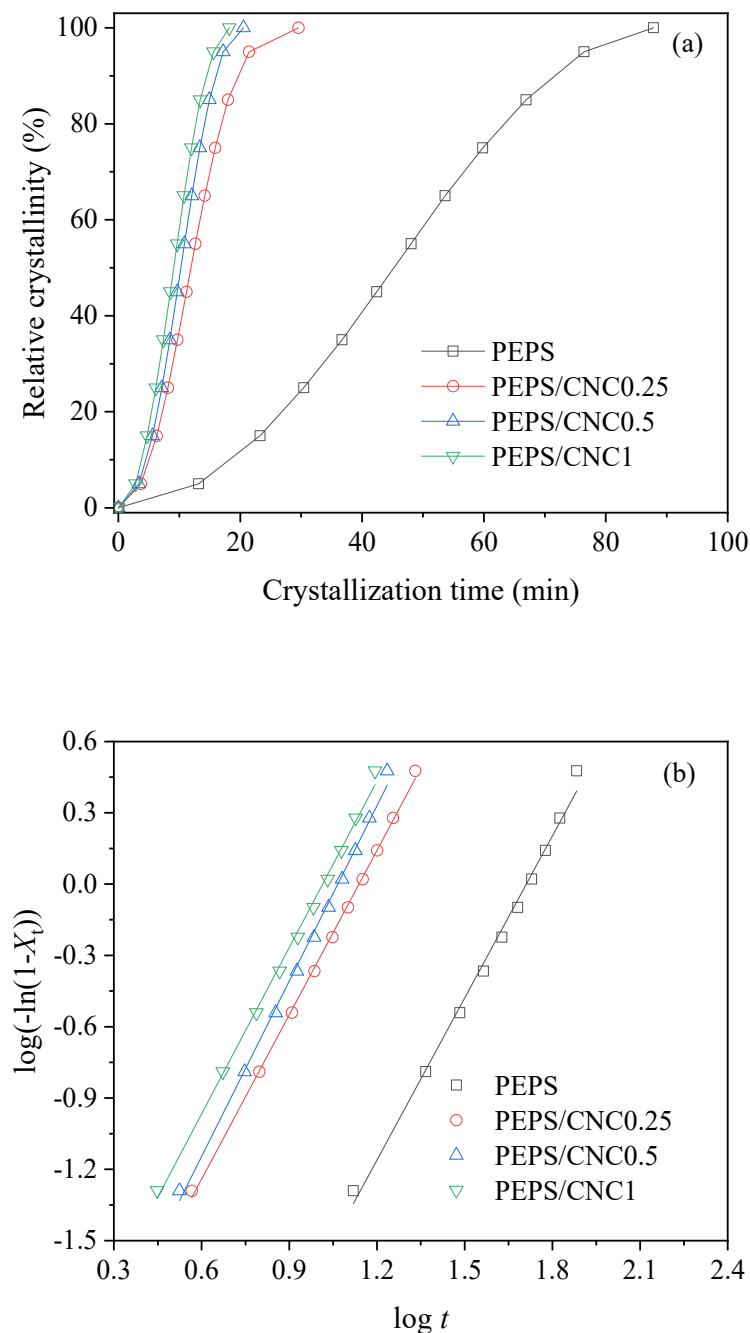


Figure 4. (a) Plots of relative crystallinity with crystallization time and (b) Avrami plots for PEPS and PEPS/CNC composites at 71 °C.

The well-known Avrami equation was utilized to analyze the isothermal crystallization kinetics of PEPS and PEPS/CNC composites. Relative crystallinity shows a relationship with crystallization time as follows:

$$1 - X_t = \exp(-kt^n) \quad (1)$$

where X_t is the relative crystallinity at crystallization time (t), k is the crystallization rate constant, and n is the Avrami exponent [41–46]. Figure 4b depict the related Avrami plots at 71 °C, showing almost parallel fitting lines for PEPS and PEPS/CNC composites, from which the n and k values were obtained. PEPS and PEPS/CNC showed similar results when they were crystallized at other T_c values. For simplicity, they are not shown here. Table 1 summarize the related isothermal crystallization kinetics parameters for PEPS and PEPS/CNC composites in the investigated T_c range.

Table 1. Isothermal crystallization kinetics parameters for PEPS and PEPS/CNC composites.

Samples	T_c (°C)	n	k (min ⁻ⁿ)	$t_{0.5}$ (min)	$t_{1/2}$ (min)
PEPS	63	2.1	1.94×10^{-3}	16.4	16.0
	65	2.2	8.90×10^{-4}	20.6	20.0
	67	2.2	5.71×10^{-4}	25.2	26.7
	69	2.2	3.10×10^{-4}	33.3	32.1
	71	2.3	1.30×10^{-4}	41.8	45.1
PEPS/CNC0.25	63	2.6	2.81×10^{-2}	3.4	3.5
	65	2.5	2.30×10^{-2}	3.9	4.2
	67	2.5	7.90×10^{-3}	6.0	6.2
	69	2.4	6.37×10^{-3}	7.1	8.4
	71	2.3	2.38×10^{-3}	11.8	11.8
PEPS/CNC0.5	63	2.6	4.19×10^{-2}	2.9	2.9
	65	2.7	1.82×10^{-2}	3.8	3.9
	67	2.6	8.43×10^{-3}	5.5	5.3
	69	2.4	7.30×10^{-3}	6.7	7.1
	71	2.4	2.39×10^{-3}	10.6	10.2
PEPS/CNC1	63	2.8	3.72×10^{-2}	2.8	2.7
	65	2.6	2.68×10^{-2}	3.5	3.5
	67	2.4	1.90×10^{-2}	4.5	4.6
	69	2.3	1.52×10^{-2}	5.3	5.9
	71	2.3	4.30×10^{-3}	9.1	9.0

From Table 1, the n values were between 2 and 3 for PEPS and PEPS/CNC composites, indicating that CNC did not change the crystallization mechanism of PEPS within the investigated T_c range. For both PEPS and PEPS/CNC composites, increasing T_c gradually decreased the k values, suggesting that the crystallization rate became slower with the increase of T_c . The k values gradually increased with increasing CNC content at the same T_c , indicating that the crystallization rate of PEPS became faster due to the nucleating agent role of CNC. It should be emphasized that the unit of k values was min⁻ⁿ, while the n values varied slightly with T_c and CNC content for PEPS and PEPS/CNC composites. Therefore, for an accurate comparison of the crystallization rate in this research, crystallization half-time ($t_{0.5}$) with the same unit (min) was used. Through the Avrami equation, $t_{0.5}$ was calculated as follows using the n and k values listed in Table 1:

$$t_{0.5} = \left(\frac{\ln 2}{k}\right)^{1/n} \quad (2)$$

The acquired $t_{0.5}$ values are summarized in Table 1, too. As displayed in Table 1, $t_{0.5}$ increased with T_c for both PEPS and PEPS/CNC composites, indicating a slower crystallization rate; moreover, $t_{0.5}$ of PEPS/CNC composites gradually decreased with increasing

CNC content, suggesting the increased crystallization rate. In addition, crystallization half-time ($t_{1/2}$) could also be directly read from the plots of relative crystallinity versus crystallization time (Figure 4a), which are also summarized in Table 1 for comparison. It is obvious that the difference between $t_{0.5}$ and $t_{1/2}$ is very small, indicating that the Avrami equation may well fit the crystallization kinetics of these systems in this research.

Crystallization rate may easily be described by the reciprocal of $t_{0.5}$ ($1/t_{0.5}$) with the same unit (min^{-1}) in polymer crystallization. The greater the $1/t_{0.5}$, the faster the crystallization rate. To show the effect of T_c and CNC content on the crystallization rate more clearly, Figure 5 demonstrate the variation of $1/t_{0.5}$ with T_c for all samples. On the one hand, $1/t_{0.5}$ increased with decreasing T_c for each sample, suggesting the faster crystallization rate due to the larger degree of supercooling. On the other hand, the $1/t_{0.5}$ values of PEPS/CNC composites were remarkably greater than that of PEPS at the same T_c and became gradually greater with increasing CNC content. The above result revealed that CNC, as an effective heterogeneous nucleating agent, obviously enhanced the crystallization rate of PEPS

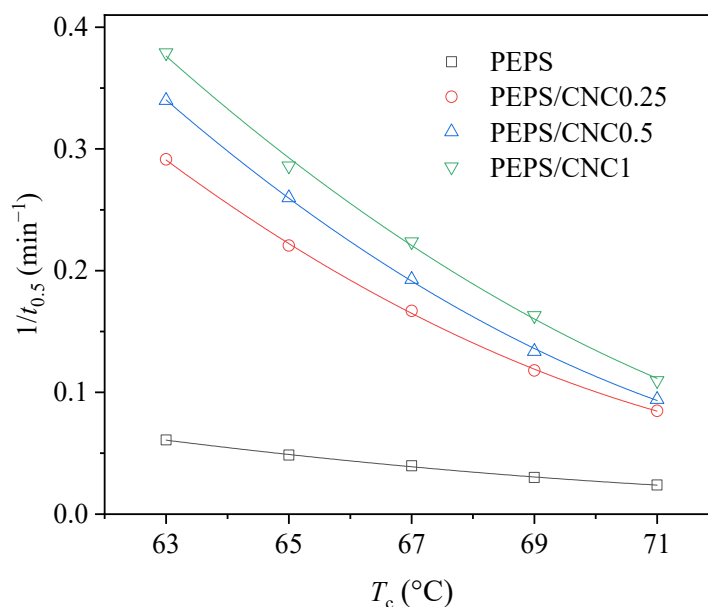


Figure 5. Variation of $1/t_{0.5}$ with T_c for PEPS and PEPS/CNC composites.

As mentioned above, CNC remarkably enhanced the crystallization behavior of PEPS under different crystallization conditions, indicating the nucleating agent role of CNC. In this section, the spherulitic morphology of PEPS and PEPS/CNC composites was directly observed with a hot-stage POM. Figure 6 illustrate the POM micrographs after PEPS and PEPS finished the crystallization at 63 °C and filled the entire space. In Figure 6a, several relatively large negative spherulites were observed for the unmodified PEPS due to the small degree of supercooling. In the case of the composites, as shown in the rest of Figure 6, the negative PEPS spherulites were still found. CNC significantly increased the number of PEPS spherulites and accordingly reduced the size of spherulites, suggesting the efficient nucleating agent role. Furthermore, the higher the CNC content, the stronger the nucleating agent effect. Despite the variation of CNC content, the spherulitic growth rates of PEPS and PEPS/CNC composites were about 2.60 $\mu\text{m}/\text{min}$. In other words, CNC only increased the nucleation density of PEPS spherulites and did not influence the growth rate. In brief, the crystalline morphology study directly confirmed that CNC enhanced the crystallization of PEPS as an outstanding heterogeneous nucleating agent by increasing the nucleation density of PEPS spherulites in the composites.

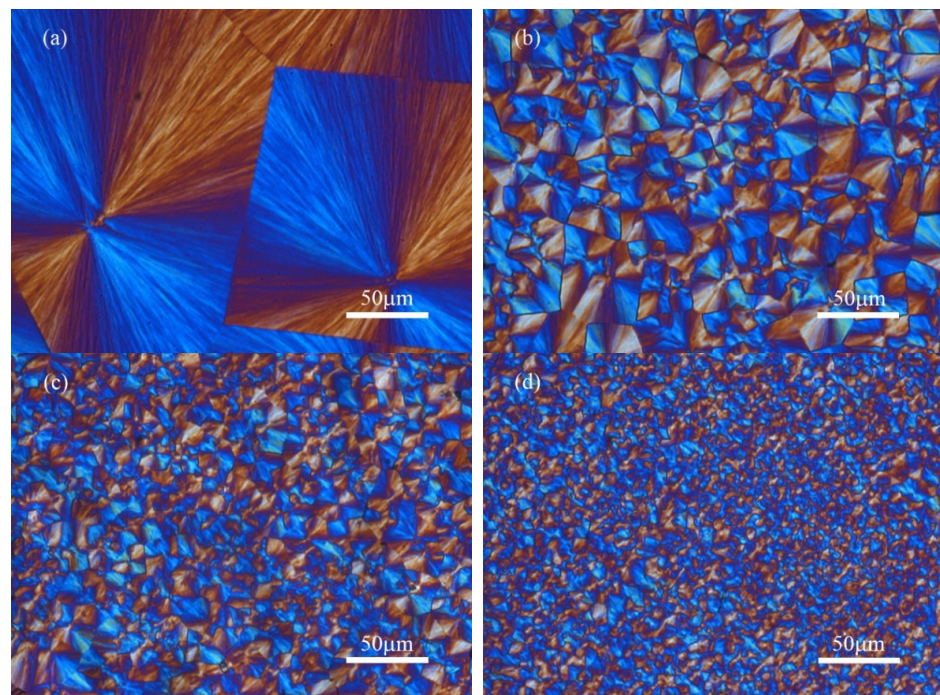


Figure 6. POM micrographs for (a) PEPS, (b) PEPS/CNC0.25, (c) PEPS/CNC0.5, and (d) PEPS/CNC1 at 63 °C.

Figure 7 displays the WAXD profiles of PEPS and PEPS/CNC composites after crystallizing at 63 °C for 8 h. PEPS showed the same crystal structure as the PES homopolymer, presenting three main diffraction peaks at 2θ of 20.3°, 22.9°, and 23.5°, which were attributed to (021), (121), and (200) planes, respectively [14,47]. In the case of the composites, they demonstrated similar WAXD profiles as PEPS, despite CNC content, suggesting that both the composites and PEPS shared the same crystal structure. From the WAXD profiles of Figure 7, the crystallinity values were calculated to be $54 \pm 2\%$ for PEPS and PEPS/CNC composites by separating the crystalline region and amorphous region of the WAXD profile in Figure 7. In brief, the crystal structure and crystallinity of PEPS remained unchanged in the composites despite the presence of CNC.

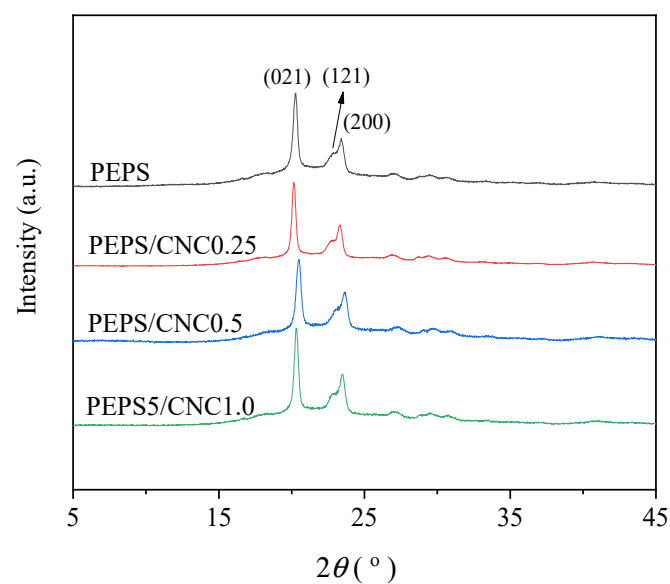


Figure 7. WAXD patterns of PEPS and PEPS/CNC composites.

From the above studies, CNC enhanced the crystallization of PEPS during both nonisothermal and isothermal melt crystallization processes. As an effective heterogeneous nucleating agent, CNC only promoted the nucleation density and hardly influenced the spherulitic growth rate of PEPS spherulites. It is interesting to discuss the effect of CNC on the enhanced nucleation density of PEPS spherulites from the viewpoint of the interfacial energy (γ_{12}) between CNC and PEPS. In the literature, the γ_{12} value between filler and polymer matrix may be calculated through the well-known harmonic mean equation or the geometric mean equation described as follows [48]:

$$\gamma_{12} = \gamma_1 + \gamma_2 - 4\left(\frac{\gamma_1^d \gamma_2^d}{\gamma_1^d + \gamma_2^d} + \frac{\gamma_1^p \gamma_2^p}{\gamma_1^p + \gamma_2^p}\right) \quad (3)$$

$$\gamma_{12} = \gamma_1 + \gamma_2 - 2\left(\sqrt{\gamma_1^d \gamma_2^d} + \sqrt{\gamma_1^p \gamma_2^p}\right) \quad (4)$$

where γ_1 and γ_2 are the surface energy of the two components, i.e., CNC and PEPS, respectively, in this work; γ^d and γ^p are dispersive components and the polar component of each component, respectively. As PEPS is a new biodegradable polymer, we calculated the surface energy, dispersive component, and polar component through the contact angle measurements using water and ethylene glycol as the solvent according to the classical method proposed by Owens and Wendt [49]. For simplicity, the details are not described here. The calculated values of PEPS are listed in Table 2. In addition, the relevant values of CNC reported in the literature are also listed in Table 2 for the calculation of γ_{12} [50].

Table 2. Surface energy data of PEPS and CNC.

Samples	γ (mN/m)	γ^d (mN/m)	γ^p (mN/m)
PEPS	31.1	14.5	16.7
CNC	60.7	39.4	21.3

On the basis of the data listed in Table 2, the γ_{12} values were calculated to be 11.96 or 6.28 mJ/m² through Equation (3) or (4), respectively. The relatively small γ_{12} value indicated a good interfacial affinity between PEPS and CNC. Consequently, CNC may not only provide sufficient active heterogeneous nucleation sites for PEPS chain to nucleate and grow on the surface but also lower the nucleation barrier, thereby increasing the nucleation rate and further overall crystallization rate.

4. Conclusions

In this research, low contents of CNC nucleated PEPS composites were successfully prepared through a solution and casting method with the aim of increasing the crystallization rate of PEPS for its potential practical application. CNC slightly increased the thermal stability of PEPS. Under both nonisothermal and isothermal melt crystallization conditions, CNC promoted the crystallization of PEPS. At a fast cooling rate of 20 °C/min, PEPS could not crystallize during the crystallization process, showing no crystallization exotherm, while PEPS/CNC composites showed well-defined crystallization exotherms. For instance, 1 wt% of CNC nucleated PEPS showed a melt crystallization temperature of 35.5 °C with a melt crystallization enthalpy of 54.6 J/g, indicating the efficient nucleating agent effect of CNC. Due to the small degree of supercooling, the crystallization half-time gradually became shorter for the unmodified and nucleated PEPS at higher crystallization temperatures. At the same crystallization temperature, CNC remarkably shortened the crystallization half-time and increased the crystallization rate of PEPS; furthermore, the higher the CNC content, the faster the crystallization rate. For example, 1 wt% of CNC significantly decreased the crystallization half-time of PEPS from 16.4 to 2.8 min. The crystalline morphology and crystal structure studies indicated that CNC did not change the growth rate and crystal structure of PEPS but increased the nucleation density of PEPS spherulites. On the basis of the harmonic mean equation or the geometric mean equation,

the interfacial energy of PEPS-CNC was determined to be 11.96 or 6.28 mJ/m², respectively. The small interfacial energy proved the good affinity between the PEPS chain and CNC surface. In other words, the PEPS chain should be easier to attach, nucleate, and further grow on the surface of CNC; therefore, CNC, as an efficient, biodegradable heterogeneous nucleating agent, significantly enhanced the crystallization of PEPS.

Author Contributions: S.P., investigation; writing—original draft preparation; Z.J., supervision; Z.Q., supervision; writing—review and editing; funding acquisition. All authors have read and agreed to the published version of the manuscript.

Funding: This research was funded by National Natural Science Foundation, China (51573016, 51521062 and 52173019).

Institutional Review Board Statement: Not applicable.

Informed Consent Statement: Not applicable.

Data Availability Statement: The data presented in this study are available on request from the corresponding author.

Acknowledgments: The authors would like to thank the National Natural Science Foundation, China (51573016, 51521062, and 52173019) for the financial support of this research.

Conflicts of Interest: The authors declare no conflict of interest.

References

1. Rhim, J.; Park, H.; Ha, C. Bio-nanocomposites for food packaging applications. *Prog. Polym. Sci.* **2013**, *38*, 1629–1652. [[CrossRef](#)]
2. Reddy, M.; Vivekanandhan, S.; Misra, M.; Bhatia, S. Mohanty, Biobased plastics and bionanocomposites: Current status and future opportunities. *Prog. Polym. Sci.* **2013**, *38*, 1653–1689. [[CrossRef](#)]
3. Gandini, A.; Lacerda, T. From monomers to polymers from renewable resources: Recent advances. *Prog. Polym. Sci.* **2015**, *48*, 1–39. [[CrossRef](#)]
4. Tadahisa, I. Biodegradable and biobased polymers: Future prospects of eco-friendly plastics. *Angew. Chem. Int. Ed.* **2015**, *54*, 3210–3215.
5. Zhu, Y.; Romain, C.; Williams, C.K. Sustainable polymers from renewable resources. *Nature* **2016**, *540*, 354–362. [[CrossRef](#)]
6. Mohanty, A.; Vivekanandhan, S.; Pin, J.; Misra, M. Composites from renewable and sustainable resources: Challenges and innovations. *Science* **2018**, *362*, 536–542. [[CrossRef](#)]
7. Ray, S.S.; Makhatha, M.E. Thermal properties of poly(ethylene succinate) nanocomposite. *Polymer* **2009**, *50*, 4635–4643.
8. Wang, H.; Qiu, Z. Crystallization kinetics and morphology of biodegradable poly(L-lactic acid)/graphene oxide nanocomposites: Influences of graphene oxide loading and crystallization temperature. *Thermochim. Acta* **2012**, *527*, 40–46. [[CrossRef](#)]
9. Vasileiou, A.A.; Papageorgiou, G.A.; Kontopoulou, M.; Docoslis, A.; Bikiaris, D. Covalently bonded poly(ethylene succinate)/SiO₂ nanocomposites prepared by in situ polymerization. *Polymer* **2013**, *54*, 1018–1032. [[CrossRef](#)]
10. Papageorgiou, G.Z.; Terzopoulou, Z.; Achilias, D.S.; Bikiaris, D.N.; Kapnisti, M.; Gournis, D. Biodegradable poly(ethylene succinate) nanocomposites. Effect of filler type on thermal behaviour and crystallization kinetics. *Polymer* **2013**, *54*, 4604–4616. [[CrossRef](#)]
11. Jing, X.; Qiu, Z. Influence of thermally reduced graphene low-loadings on the crystallization behavior and morphology of biodegradable poly(ethylene succinate). *Ind. Eng. Chem. Res.* **2014**, *53*, 498–504. [[CrossRef](#)]
12. Asadi, V.; Jafari, S.H.; Khonakdar, A.H.; Häußler, L.; Wagenknecht, U. Incorporation of inorganic fullerene-like WS₂ into poly(ethylene succinate) to prepare novel biodegradable nanocomposites: A study on isothermal and dynamic crystallization. *RSC Adv.* **2016**, *6*, 4925–4935. [[CrossRef](#)]
13. Teng, S.; Qiu, Z. Effect of different POSS structures on the crystallization behavior and dynamic mechanical properties of biodegradable poly(ethylene succinate). *Polymer* **2019**, *163*, 68–73. [[CrossRef](#)]
14. Zhang, K.; Qiu, Z. Effect of methyl as the simplest C–H side group on the significant variation of physical properties of biodegradable poly(ethylene succinate). *Polym. Test.* **2020**, *90*, 106755. [[CrossRef](#)]
15. Lu, H.; Lu, S.; Chen, M.M. Characterization, crystallization kinetics, and melting behavior of poly(ethylene succinate) copolyester containing 7 mol% butylene succinate. *J. Appl. Polym. Sci.* **2009**, *113*, 876–886. [[CrossRef](#)]
16. Chen, M.; Chang, W.; Lu, H. Characterization, crystallization kinetics and melting behavior of poly(ethylene succinate) copolyester containing 5 mol% trimethylene succinate. *Polymer* **2007**, *48*, 5408–5416. [[CrossRef](#)]
17. Li, X.; Qiu, Z. Crystallization kinetics, morphology, and mechanical properties of novel poly(ethylene succinate-co-octamethylene succinate). *Polym. Test.* **2015**, *48*, 125–132. [[CrossRef](#)]
18. Li, X.; Qiu, Z. Synthesis and properties of novel poly(ethylene succinate-co-decamethylene succinate) copolymers. *RSC Adv.* **2015**, *5*, 103713–103721. [[CrossRef](#)]

19. Wu, H.; Qiu, Z. Synthesis, crystallization kinetics and morphology of novel poly(ethylene succinate-co-ethylene adipate) copolymer. *CrystEngComm* **2012**, *14*, 3586–3595. [[CrossRef](#)]
20. Qiu, S.; Su, Z.; Qiu, Z. Crystallization kinetics, morphology and mechanical properties of novel biodegradable poly(ethylene succinate-co-ethylene suberate) copolyesters. *Ind. Eng. Chem. Res.* **2016**, *55*, 10286–10293. [[CrossRef](#)]
21. Qiu, S.; Zhang, K.; Su, Z.; Qiu, Z. Thermal behavior, mechanical and rheological properties, and hydrolytic degradation of novel branched biodegradable poly(ethylene succinate) copolymers. *Polym. Test.* **2018**, *66*, 64–69. [[CrossRef](#)]
22. Zhang, K.; Qiu, Z. Miscibility and crystallization behavior of novel branched poly(ethylene succinate)/poly(vinyl phenol) blends, Chinese. *J. Polym. Sci.* **2019**, *37*, 1169–1175.
23. Zhang, K.; Qiu, Z. Effect of cyanuric acid as an efficient nucleating agent on the crystallization of novel biodegradable branched poly(ethylene succinate). *Macromol* **2021**, *1*, 112–120. [[CrossRef](#)]
24. Zhang, K.; Jiang, Z.; Qiu, Z. Effect of different lengths of side groups on the thermal, crystallization and mechanical properties of novel biodegradable poly(ethylene succinate) copolymers. *Polym. Degrad. Stabil.* **2021**, *187*, 109542. [[CrossRef](#)]
25. Habibi, Y.; Lucia, L.A.; Rojas, O.J. Cellulose Nanocrystals: Chemistry, Self-Assembly, and Applications. *Chem. Rev.* **2010**, *110*, 3479–3500. [[CrossRef](#)] [[PubMed](#)]
26. Ferreira, F.; Dufresne, A.; Pinheiro, I.; Souza, D.; Gouveia, R.; Mei, L.; Lona, L. How do cellulose nanocrystals affect the overall properties of biodegradable polymer nanocomposites: A comprehensive review. *Eur. Polym. J.* **2018**, *108*, 274–285. [[CrossRef](#)]
27. Younas, M.; Noreen, A.; Sharif, A.; Majeed, A.; Hassan, A.; Tabasum, S.; Mohammadi, K.; Zia, K.M. A review on versatile applications of blends and composites of CNC with natural and synthetic polymers with mathematical modeling. *Int. J. Biol. Macromol.* **2019**, *124*, 591–626. [[CrossRef](#)]
28. Calvino, C.; Macke, N.; Kato, R.; Rowan, S. Development, processing and applications of bio-sourced cellulose nanocrystal composites. *Prog. Polym. Sci.* **2020**, *103*, 101221. [[CrossRef](#)]
29. Li, Y.; Han, C.; Yu, Y.; Xiao, L. Effect of loadings of nanocellulose on the significantly improved crystallization and mechanical properties of biodegradable poly(ϵ -caprolactone). *Int. J. Biol. Macromol.* **2020**, *147*, 34–45. [[CrossRef](#)]
30. Kamal, M.; Khoshkava, V. Effect of cellulose nanocrystals (CNC) on rheological and mechanical properties and crystallization behavior of PLA/CNC nanocomposites. *Carbohydr. Polym.* **2015**, *123*, 105–114. [[CrossRef](#)]
31. Xu, C.; Lv, Q.; Wu, D.; Wang, Z. Polylactide/cellulose nanocrystal composites: A comparative study on cold and melt crystallization. *Cellulose* **2017**, *24*, 2163–2175. [[CrossRef](#)]
32. Li, J.; Qiu, Z. Significantly enhanced crystallization of poly(L-lactide) by the synergistic effect of poly(diethylene glycol adipate) and cellulose nanocrystals in their fully biodegradable ternary composite. *Ind. Eng. Chem. Res.* **2019**, *58*, 15526–15532. [[CrossRef](#)]
33. Li, Y.; Fu, Q.; Wang, M.; Zeng, J. Morphology, crystallization and rheological behavior in poly(butylene succinate)/cellulose nanocrystal nanocomposites fabricated by solution coagulation. *Carbohydr. Polym.* **2017**, *164*, 75–82. [[CrossRef](#)]
34. Clarke, A.; Vasileiou, A.; Kontopoulou, M. Crystalline nanocellulose/thermoplastic polyester composites prepared by in situ polymerization. *Polym. Eng. Sci.* **2019**, *59*, 989–995. [[CrossRef](#)]
35. Li, J.; Jiang, Z.; Qiu, Z. Thermal and rheological properties of fully biodegradable poly(ethylene succinate)/cellulose nanocrystals composites. *Compos. Commun.* **2021**, *23*, 100571. [[CrossRef](#)]
36. Li, J.; Jiang, Z.; Qiu, Z. Isothermal melt crystallization kinetics study of cellulose nanocrystals nucleated biodegradable poly(ethylene succinate). *Polymer* **2021**, *227*, 123869. [[CrossRef](#)]
37. Li, J.; Qiu, Z. Nonisothermal melt crystallization study of poly(ethylene succinate)/cellulose nanocrystals composites. *J. Polym. Environ.* **2021**. [[CrossRef](#)]
38. Pan, S.; Qiu, Z. Fully biodegradable poly(hexamethylene succinate)/cellulose nanocrystals composites with enhanced crystallization rate and mechanical property. *Polymers* **2021**, *13*, 3667. [[CrossRef](#)]
39. Li, J.; Qiu, Z. Effect of low loadings of cellulose nanocrystals on the significantly enhanced crystallization of biodegradable poly(butylene succinate-co-butylene adipate). *Carbohydr. Polym.* **2019**, *205*, 211–216. [[CrossRef](#)]
40. Li, J.; Qiu, Z. Influence of two different nanofillers on the crystallization behavior and dynamic mechanical properties of biodegradable poly(ethylene adipate). *J. Polym. Environ.* **2019**, *27*, 2674–2681. [[CrossRef](#)]
41. Avrami, M. Kinetics of phase change. II Transformation-time relations for random distribution of nuclei. *J. Chem. Phys.* **1940**, *8*, 212–224. [[CrossRef](#)]
42. Avrami, M. Granulation, phase change, and microstructure kinetics of phase change III. *J. Chem. Phys.* **1941**, *9*, 177–184. [[CrossRef](#)]
43. Teng, S.; Jiang, Z.; Qiu, Z. Crystallization behavior and dynamic mechanical properties of poly(ϵ -caprolactone)/octaisobutyl-polyhedral oligomeric silsesquioxanes composites prepared via different methods. *Chin. J. Polym. Sci.* **2020**, *38*, 158–163. [[CrossRef](#)]
44. Zhou, M.; Zhang, K.; Jiang, Z.; Qiu, Z. Synthesis and characterization of novel poly(butylene succinate)-*b*-poly(diethylene glycol terephthalate) multiblock copolyesters with high melting point and significantly improved mechanical property. *Polymer* **2021**, *232*, 124151. [[CrossRef](#)]
45. Yang, F.; Qiu, Z. Preparation, crystallization and properties of biodegradable poly(butylene adipate-co-terephthalate)/organo-modified montmorillonite nanocomposites. *J. Appl. Polym. Sci.* **2011**, *119*, 1426–1434. [[CrossRef](#)]
46. Xu, C.; Qiu, Z. Crystallization behavior and thermal property of biodegradable poly(3-hydroxybutyrate)/multi-walled carbon nanotubes nanocomposite. *Polym. Adv. Technol.* **2011**, *22*, 538–544. [[CrossRef](#)]

47. Ueda, A.S.; Chatani, Y.; Tadokoro, H. Structure studies of polyesters. IV. Molecular and crystal structure of poly(ethylene succinate) and poly(ethylene oxalate). *Polym. J.* **1971**, *2*, 387–397. [[CrossRef](#)]
48. Wu, S. *Polymer Interface and Adhesion*; Marcel Dekker: New York, NY, USA, 1982.
49. Owens, D.K.; Wendt, R.C. Estimation of surface free energy of polymers. *J. Appl. Polym. Sci.* **1969**, *13*, 1741–1747. [[CrossRef](#)]
50. Lin, N.; Huang, J.; Chang, P.R.; Feng, J.; Yu, J. Surface acetylation of cellulose nanocrystal and its reinforcing function in poly(lactic acid). *Carbohydr. Polym.* **2011**, *83*, 1834–1842. [[CrossRef](#)]